Electrochemistry Communications 125 (2021) 106992

Contents lists available at ScienceDirect

Electrochemistry Communications

journal homepage: www.elsevier.com/locate/elecom

Short Communication

'Dry' electrochemistry: A non-invasive approach to the characterization of archaeological iron objects

Antonio Doménech-Carbó [a,*], María Amparo Peiró-Ronda [b], Jaime Vives-Ferrándiz [b], Gustavo S. Duffó [c,d,e], Silvia Farina [c,d,e]

[a] Department of Analytical Chemistry, Universitat de València, Dr. Moliner 50, 46100 Burjassot, Valencia, Spain
[b] Servicio de Investigación Prehistórica, Museu de Prehistòria de València, Corona 36, 46003 Valencia, Spain
[c] Comisión Nacional de Energía Atómica, Av. Gral. Paz 1499, (1650) San Martín, Argentina
[d] Consejo Nacional de Investigaciones Científicas y Técnicas, Godoy Cruz 2290, (1525) Buenos Aires, Argentina
[e] Universidad Nacional de San Martín, 25 de Mayo y Francia, San Martín (1650), Argentina

ARTICLE INFO

Keywords:
Archaeology
Iron
Open circuit potential
Electrochemistry

ABSTRACT

A methodology for monitoring the corrosion state of archaeological iron objects using 'dry' open circuit potential (OCP) measurements is described. Application of this technique to a set of objects from La Bastida de les Alcusses archaeological site (Moixent, València, Spain), dating back to the 4th century BCE, reveals significant differences depending on the conservation state. The transient OCP responses (which last between a few seconds and 10–15 min) were superimposed with much shorter (less than one second) intense features.

1. Introduction

The corrosion of iron artifacts is a recurring problem in archaeology, conservation and restoration sciences. Due to the porous nature of the corrosion products, the surface corrosion of iron artifacts may progress continuously until the metal core is completely mineralized [1]. In the initial steps of this process the objects roughly maintain their original shape and size, then eventually lose their shape through the progressive appearance of deforming corrosion products [2]. Thus, non-destructive techniques for monitoring the degradation state of artifacts and the performance of various stabilization/desalination/coating procedures are attracting increasing attention [3–6].

In this context, various techniques such as Kelvin probe microscopy, electrochemical noise and electrochemical impedance spectroscopy (EIS) using non-aggressive aqueous electrolytes [4,7], and jellified electrolytes [3,5,6] can be used to acquire information on the composition, roughness, porosity, etc. of corrosion layers. However, the application of such techniques to the routine analysis of archaeological objects is often difficult due to the need for relatively sophisticated instrumentation and/or data treatment, and/or the potentially destructive treatment of the objects. Open circuit potential (OCP) measurements have also been used to characterize metallic materials [8] and to evaluate corrosion in steel bars embedded in concrete [9,10]. These latter methods, directly inspired by the standardized method of the American Society for Testing and Materials (ASTM) [11] involve the use of a reference electrode (typically $Cu/CuSO_4$) connected to the concrete surface by a wet sponge or paper [9–11].

Although the use of jellified electrolytes can minimize the problems associated with such wet contacts, the application of these methodologies to archaeological iron objects with a high level of mineralization is difficult. In this report, we present a "dry" electrochemical methodology which involves recording the potential difference between two points on the object, one of which corresponds to the metallic core or the conducting metal oxides surface. The variation of the measured "dry" potential difference (V_D) with time (t) has been studied for archaeological iron objects from the La Bastida de les Alcusses archaeological site (Moixent, València, Spain), which date back to the 4th century BCE, including pristine artifacts and objects subjected to different stabilization/desalination procedures. The resulting V_D vs. t curves consist of longer (between a few seconds and 10–15 min) transients with superimposed short (less than one second) intense features. These last have a certain resemblance to single nanoparticle collision events [12–14] and experiments monitoring metal pitting corrosion under open circuit potential conditions [15].

* Corresponding author.
E-mail address: antonio.domenech@uv.es (A. Doménech-Carbó).

https://doi.org/10.1016/j.elecom.2021.106992
Received 9 February 2021; Received in revised form 25 February 2021; Accepted 25 February 2021
Available online 7 March 2021

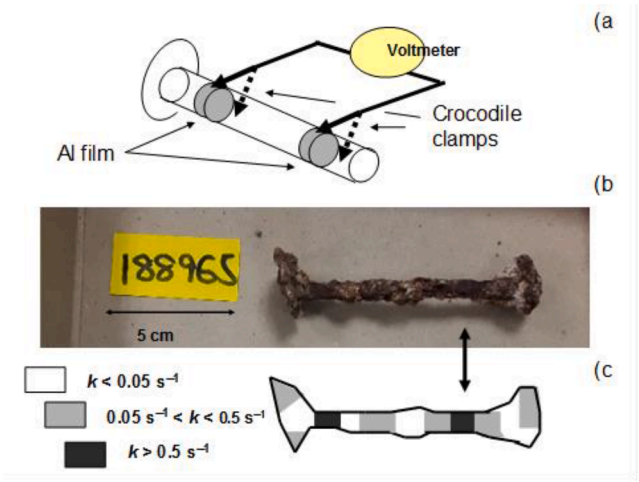

Fig. 1. (a) Schematic illustration of the "dry" electrochemistry measurement system; (b) photographic image of a highly altered nail from La Bastida archaeological site (cat. n. 188965); (c) mapping of surface corrosion level according to the values of the rate constant k described in the text. The double arrow marks the point of connection with the reference terminal of the potentiostat.

2. Experimental

2.1. Samples

The samples consisted of 8 nails recovered from La Bastida de les Alcusses archaeological site. All these objects were 12 ± 1 cm in length and were recovered under burial conditions during ordinary archaeological excavations. Since their discovery in 2010 they have been stored in the repository of the Museu de Prehistòria de València (Spain). These include pristine nails (cat. n. 188887, 188912, 188965, 188972) and nails previously subjected to various alkaline desalination treatments aimed at stabilization (cat. n. 188885, 188960, 188966, 188973). Complementary experiments were performed with contemporary stainless steel nails. These were selected for their high accessibility and passive surface combined with highly uniform conducting properties.

2.2. OCP measurements

V_D measurements on the stainless steel nails and archaeological artifacts were made in two rounds, one in the Prehistory Museum of Valencia at 20 °C and 70% RH and the second in the university laboratories at 18 °C and 75% RH. The former were carried out with IVIUM portable equipment and the second with a CH 660I potentiostat connecting the reference and working electrode terminals through crocodile clamps to two selected points on the object. Control experiments were carried out with a hemi-cylindrical Faraday cage (25 × 7.5 cm in size) in order to test the possible influence of external electrical sources. To prevent mechanical degradation of the object, two aluminum foils 5 mm in width were interposed between the object and the connection clamps, as shown schematically in Fig. 1(a). The distance between the contact points of the artifacts was always between 1.0 and 5.0 cm. The reference electrode terminal was connected to a region of the object exhibiting apparently low corrosion (see Fig. 1b for a highly corroded nail cat. n. 188965). Here, conducting corrosion products will ensure electrical conductivity. The working electrode terminal was connected to the problem region. This makes it possible to map the corrosion level of different areas of the artifact surface, as depicted in Fig. 1(c). Complementary ATR-FTIR and voltammetric experiments were performed to identify corrosion products as described previously [16].

3. Results and discussion

Fig. 2 shows V_D vs. time curves recorded for a contemporary stainless steel nail (a) and two nails from La Bastida archaeological site (b–d). One of these nails had been previously subjected to a stabilizing protocol with NaOH (3% wt) plus tannic acid (5% wt) solution (c) while the other remained untreated (b, d). In all cases, V_D varied with time following an exponential variation (*vide infra*) tending to a constant value after times ranging between a few seconds and 2–5 min. In the case of "fresh" metal (Fig. 2(a), a contemporary stainless steel nail), V_D varied in a range of 1–5 mV whereas in the case of a stabilized iron nail (Fig. 2c), V_D ranged between 50 and 100 mV. The V_D vs. t curve was sensitive to changes in the position of the clamps and the distance between them. Our data indicated, however, that differences in the 1–5 cm separation range were minor. In the case of nails showing high corrosion (Fig. 2b, d), the V_D vs. t pattern was more sensitive to the position of the clamps. If one

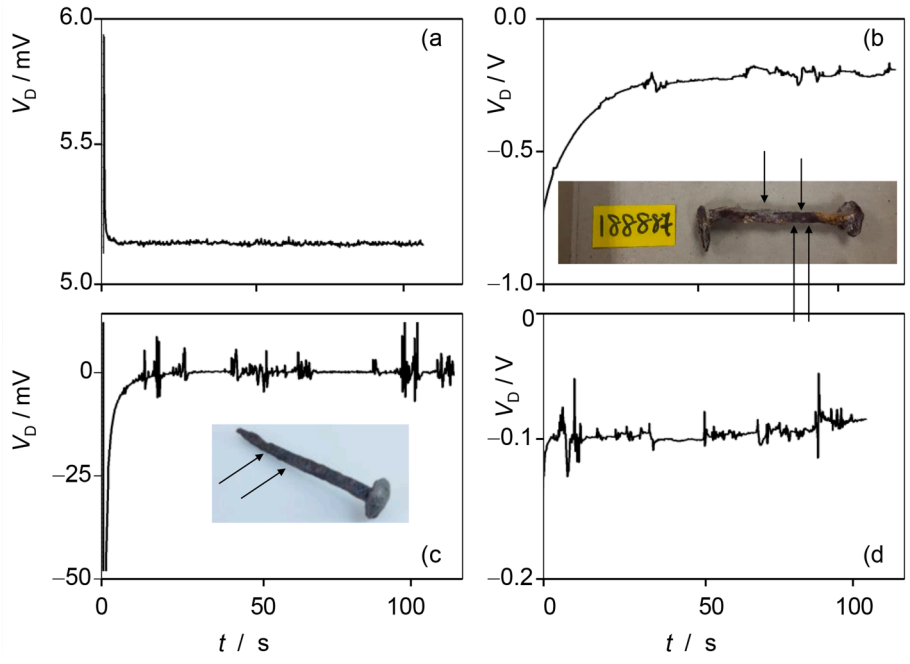

Fig. 2. V_D vs. time curves recorded for: (a) a contemporary stainless steel nail and (b–d) nails from La Bastida archaeological site (12 cm in length). Data are given for a highly altered nail cat. n. 188,887 (see photograph) connected between light and high corrosion areas (b) and between two lightly corroded areas (d). (c) Data for nail cat. n. 188960, subjected to a stabilizing protocol with NaOH (3% wt) plus tannic acid (5% wt) solution. Notice the different V_D scale in (a, c) and (b, d). The arrows mark the position of the respective connections.

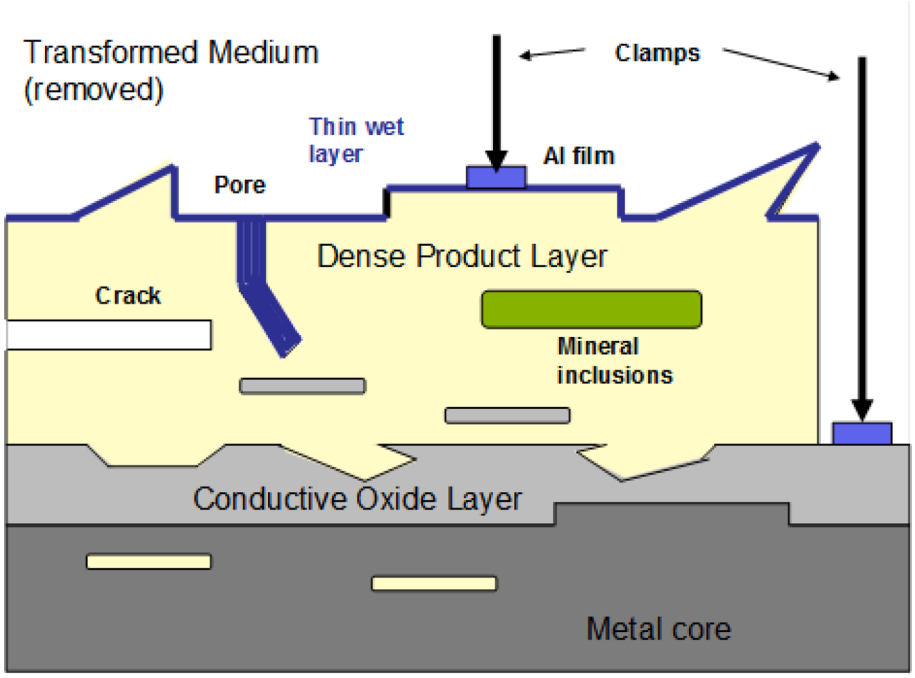

Fig. 3. Schematic description of the structure of the corrosion layers on an archaeological iron artifact found buried in soil, showing the electrical connections used in the present study.

region of light corrosion was connected to another with high corrosion (Fig. 2c, d), the measured potentials increased between 0.1 and 0.5 V, from the initial to the limiting value. The overall V_D vs. t curve shows sharp transients of different durations and intensities. No significant differences were seen between the V_D vs. time responses recorded in the museum and laboratory environments; in particular, identical transient profiles were obtained in experiments performed with and without the Faraday cage. Similarly, control experiments without interposed aluminium sheets displayed essentially identical results, thus suggesting that there are no significant capacitive effects associated with the aluminium/corrosion products interface. This is consistent with abundant EIS data suggesting that these types of effects are largely confined to the high-frequency (i.e., short time) domain, in contrast with the longer times involved in our OCP measurements. Interestingly, these transients are more marked in the case of stabilized objects and lightly corroded artifacts, as can be seen in Fig. 2.

The features of the general curves recorded for the variation of V_D with time can be fitted to an exponential equation of the form:

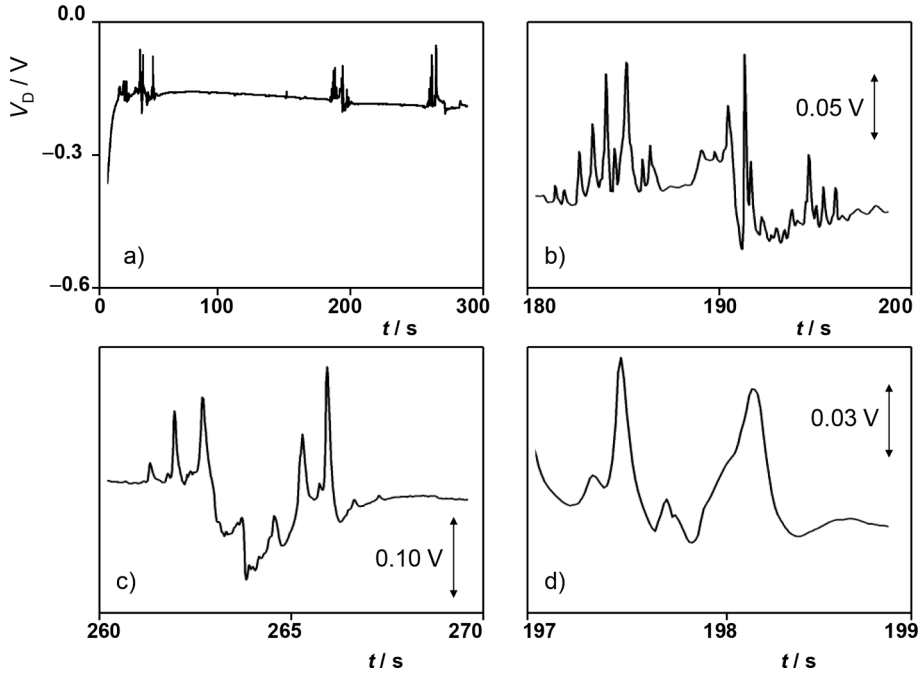

Fig. 4. V_D vs. time curves recorded for nail cat. n. 188973, subjected to a stabilizing protocol with Na_2SO_3 (63 g L^{-1}) plus NaOH (20 g L^{-1}) solution and tannic acid (5% wt) solution. Complete curve (a) and details of different time intervals showing sharp transient responses (b–d).

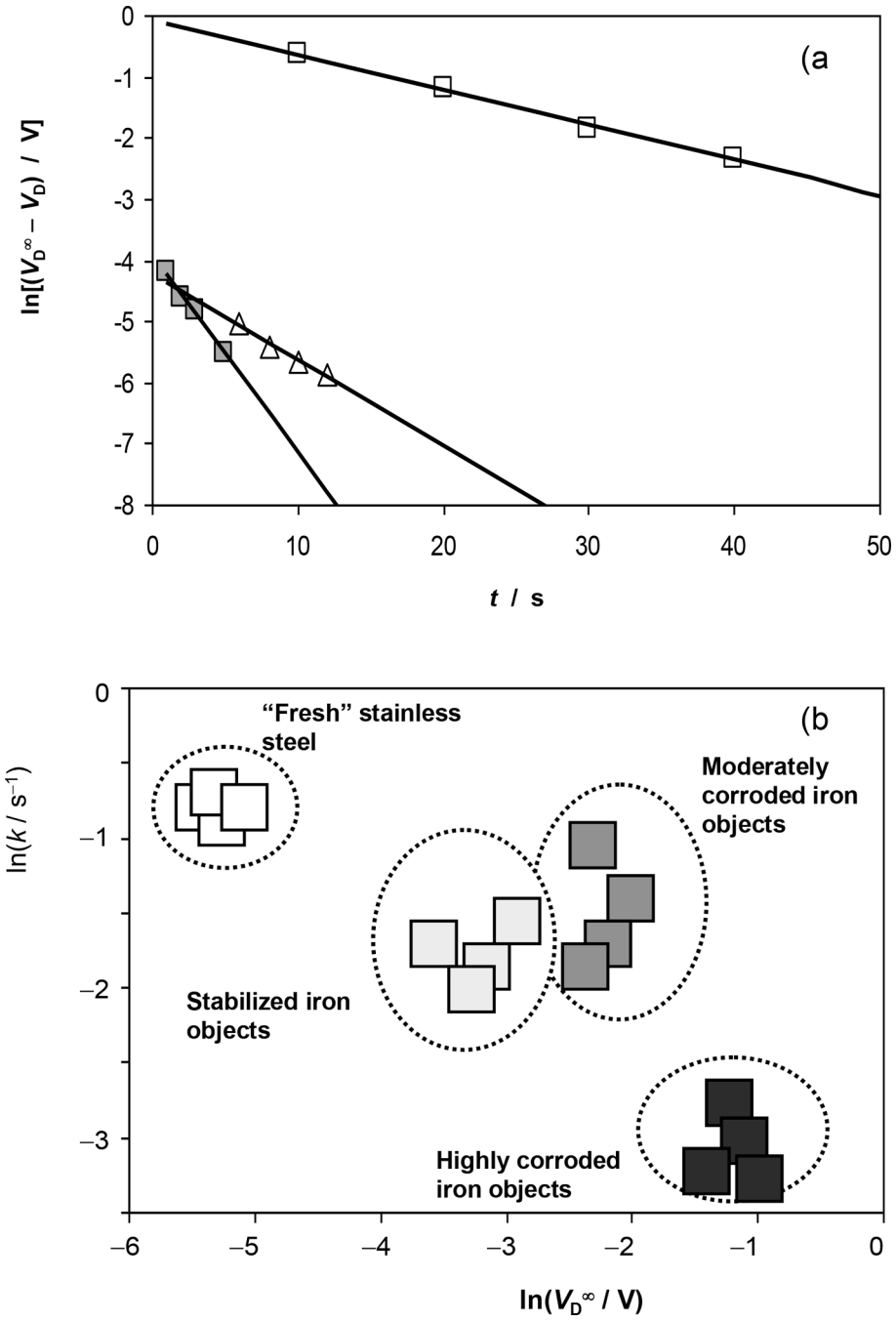

Fig. 5. (a) Plots of $ln(V_D^{\infty} - V_D)$ vs. time curves for nail cat. n. 188,887 connecting light and high corrosion areas (hollow squares) and two lightly corroded areas (solid squares) and nail cat. n. 188960, subjected to a stabilizing protocol with NaOH (3% wt) plus tannic acid (5% wt) solution (triangles). (b) Two-dimensional diagram based on the values of V_D^{∞} and k in double logarithmic scale, grouping the studied objects.

$$V_D = V_D^o + (V_D^{\infty} - V_D^o)(1 - e^{-kt}) \quad (1)$$

representative of the variation of V_D between initial (V_D^o) and limiting (V_D^{∞}) potentials corresponding to linear $ln(V_D^{\infty} - V_D)$ vs. time representations. This variation suggests that a resistive plus capacitive (RC equivalent circuit) system operates with a time constant k. Qualitatively, this variation can be interpreted using the description of Dillmann et al. [2,17] of the structure of the corrosion layers of archaeological iron objects. Here, the metal is covered by a dense product layer (DPL), composed of ferric oxyhydroxides, mainly goethite (α-FeOOH) and lepidocrocite (γ-FeOOH), which in turn is covered by a layer of transformed medium (TM) which constitutes a transition zone between the DPL and the soil. This layer contains both corrosion products and soil materials such as calcite, clays, and quartz. The metal core can be covered by a layer of conductive oxides (mainly magnetite) and the DPL can be crossed by oxide marblings (magnetite and/or maghemite), slag inclusions from the metal, as well as cracks, pores, and foreign mineral inclusions. In the case of the objects under study, ATR-FTIR and voltammetric data indicate that the conductive layer is mainly composed of magnetite while the DPL is dominated by ochre, accompanied by hematite, goethite and lepidocrocite, and also, in regions of high corrosion, by inclusions of $CaCO_3$ and clays.

In our experiments, shown schematically in Fig. 3, one clamp was connected to the conductive oxide layer and the other to the DPL. In principle, the difference in potential between the connections could be computed by considering the contribution of the difference in the work

functions of the metal and the product of metal corrosion. Since the contribution of the two clamped aluminum contacts must cancel out, V_D initially reflects the difference in potential at the metal/metal corrosion products interface, corresponding to the contact potential difference, $\varphi^{o}_{Fe-FeOx}$ [18,19]. This difference in potential will vary as a result of charge transfer through the fine humidity layer between the different solid phases which acts as an electrolyte. The time constant in Eq. (1) can be considered as representative of charging processes. Given the semiconducting nature of most corrosion products, we can consider charge transfer involving electrolyte double layer charging and space charge effects as possible contributors to the capacitive effects suggested by Eq. (1).

Fig. 4 shows V_D vs. time curves recorded for a nail (cat. n. 188973) subjected to a stabilizing protocol. Sharp transients appear at different time intervals, superimposed on the overall exponential curve. One can see that the transients exhibit different morphologies, although exponential decays in the descending branches of the peaked features predominate. These features can tentatively be attributed to charge/discharge processes associated with discontinuities in the metal patina, to some extent mimicking transient pitting corrosion phenomena [15]. Such features are particularly interesting in connection with archaeological iron because they may be associated with the porosity and compaction of the metal patina as well as the presence of chloride reservoirs which promote the long-term corrosion of the objects even after stabilizing treatment [1].

Consistent with this scheme, V_D measurements on "fresh" stainless steel nails, as well as those performed by connecting two points on metallic (or slightly corroded) archaeological objects, yield V_D values of around a few mV. Also consistent with the previous considerations, the limiting V_D values tends to clearly higher values when the conducting area is connected to moderate or highly corroded regions. Fig. 5a depicts the plots of $ln(V_D^{\infty} - V_D)$ vs. time curves recorded for a corroded nail, connecting points between light and highly corroded areas (squares) and between two lightly corroded areas (solid squares) and a stabilized nail (triangles). In all cases satisfactory linearity was obtained (regression equations $ln(V_D^{\infty} - V_D) = (0.058 \pm 0.001)t - (0.07 \pm 0.03)$, $r = 0.9996$; $ln(V_D^{\infty} - V_D) = (0.323 \pm 0.017)t - (3.90 \pm 0.05)$, $r = 0.997$; $ln(V_D^{\infty} - V_D) = (0.142 \pm 0.006)t - (4.16 \pm 0.05)$, $r = 0.998$, respectively).

These electrochemical data can be used to monitor the corrosion state of archaeological objects, prompting the mapping of regions with different degrees of corrosion. An example, based on the values of the rate constant k, is depicted in Fig. 1(c). Since the measurement of the initial potential may experience equipment bias effects, the potentials extrapolated at infinite time, V_D^{∞}, were used to characterize the different corrosion patterns. The discrimination between different typologies is illustrated in Fig. 5(b), where a two-dimensional diagram based on the values of V_D^{∞} and k is depicted in double logarithmic scale. This diagram clearly separates highly corroded and lightly corroded objects and also distinguishes objects subjected to stabilizing treatments. Remarkably, the stabilized objects differ from the "fresh" objects in the diagram. This approach opens the possibility of evaluating the efficiency of different stabilizing treatments, a matter of considerable interest in metal conservation and restoration [1,2].

4. Conclusions

Though detailed modeling of the processes involved in "dry" OCP measurements still remains to be done, these findings can be regarded as a promising tool for gaining information on the corrosion level of archaeological iron objects which is relevant for conservation and restoration purposes. The rapid and non-destructive methodology provides information on the overall corrosion state and degree of mineralization, porosity and existence of chloride reservoirs in the corrosion layers.

CRediT authorship contribution statement

Antonio Doménech-Carbó: Conceptualization. **María Amparo Peiró Ronda:** . **Jaime Vives-Ferrándiz:** . **Gustavo S. Duffó:** Formal analysis. **Silvia Farina:** Formal analysis.

Declaration of Competing Interest

The authors declare that they have no known competing financial interests or personal relationships that could have appeared to influence the work reported in this paper.

Acknowledgement

Financial support from the MINECO Project CTQ2017-85317-C2-1-P which is supported by *Ministerio de Economía, Industria y Competitividad* (MINECO) and *Fondo Europeo de Desarrollo Regional* (ERDF) funds is gratefully acknowledged. GSD and SBF acknowledge support from ANPCYT Project 2016-0082, Agencia Nacional de Promoción Científica y Técnica, Argentina. Fieldwork at La Bastida de les Alcusses has been carried out under the financial support of the Museum of Prehistory (Diputación de Valencia) since 1928.

References

[1] L. Selwyn, Overview of archaeological iron: the corrosion problem, key factors affecting treatment, and gaps in current knowledge. Proc. Metal 2004, National Museum of Australia, Canberra, 2004, pp. 294-306.
[2] C. Rémazeilles, D. Neff, F. Kergourlay, E. Foy, E. Conforto, E. Guilminot, S. Reguer, P. Refait, P. Dillmann, Corros. Sci. 51 (2009) 2932–2941.
[3] E. Cano, A. Crespo, D. Lafuente, B. Ramírez-Barat, Electrochem. Commun. 41 (2014) 16–19.
[4] E. Cano, D. Lafuente, D.M. Bastidas, J. Solid State Electrochem. 14 (2010) 381–391.
[5] B. Ramírez-Barat, E. Cano, Electrochim. Acta 182 (2015) 751–762.
[6] F. Di Turo, C. De Vito, F. Coletti, F. Mazzei, R. Antiocchia, G. Favero, Microchem. J. 134 (2017) 154–163.
[7] A. Doménech-Carbó, M. Lastras, F. Rodríguez, E. Cano, J. Piquero-Cilla, L. Osete-Cortina, J. Solid State Electrochem. 18 (2014) 399–409.
[8] C. Degrigny, G. Guibert, S. Ramseyer, G. Rapp, A. Tarchini, J. Solid State Electrochem. 14 (2010) 425–435.
[9] A. Sassolini, N. Colozza, E. Papa, K. Hermansson, I. Cacciotti, F. Arduini, Electrochem. Commun. 98 (2019) 69–72.
[10] G.S. Duffó, S.B. Farina, C.M. Giordano, Electrochim. Acta 54 (2009) 1010–1020.
[11] A.S.T.M. Standard, C876: Standard Test Method for Corrosion Potentials of Uncoated Reinforcing Steel in Concrete, ASTM International, West Conshohocken, PA, 2009.
[12] E.J.F. Dickinson, N.V. Rees, R.G. Compton, Chem. Phys. Lett. 528 (2012) 44–48.
[13] W. Cheng, R.G. Compton, Trends Anal. Chem. 58 (2014) 79–89.
[14] F. Scholz, D. Hellberg, F. Harnisch, A. Hummel, U. Hasse, Electrochem. Commun. 6 (2004) 929–933.
[15] G. Berthomé, B. Malki, B. Baroux, Corros. Sci. 48 (2006) 2432–2441.
[16] A. Doménech-Carbó, M. Lastras, F. Rodríguez, L. Osete-Cortina, Mapping of corrosion products of highly altered archeological iron using voltammetry of microparticles, Microchem. J. 106 (2012) 41–50.
[17] D. Neff, P. Dillmann, M. Descostes, G. Beranger, Corros. Sci. 48 (2006) 2947–2970.
[18] M.S. Venkatraman, I.S. Cole, B. Emmanuel, Corros. Sci. 56 (2011) 7171–7179.
[19] M.S. Venkatraman, I.S. Cole, B. Emmanuel, Corros. Sci. 56 (2011) 8192–8203.